Test-Photostability of pulsed laser deposited amorphous thin films from Ge-As-Te system

P. Hawlová, F. Verger, Virginie Nazabal, Rémi Boidin, P. Nemec

SCIENTIFIC REPORTS

OPEN

CONFERENCE PROCEEDINGS

ISFM2014

SUBJECT AREAS:

MATERIALS FOR OPTICS

OPTICAL MATERIALS AND STRUCTURES

Received
18 September 2014

Accepted
16 December 2014

Published
23 March 2015

Correspondence and requests for materials should be addressed to P.N. (petr.nemec@upce.cz)

Photostability of pulsed laser deposited amorphous thin films from Ge-As-Te system

P. Hawlová[1], F. Verger[1], V. Nazabal[1,2], R. Boidin[1] & P. Němec[1]

[1]Department of Graphic Arts and Photophysics, Faculty of Chemical Technology, University of Pardubice, 53210 Pardubice, Czech Republic, [2]Institut des sciences chimiques de Rennes, UMR CNRS 6226, Equipe Verres et Céramiques, Université de Rennes 1, 35042 Rennes, France.

Amorphous thin films from Ge-As-Te system were prepared by pulsed laser deposition to study their intrinsic photostability, morphology, chemical composition, structure and optical properties. Photostability of fabricated layers was studied by spectroscopic ellipsometry within as-deposited as well as relaxed (annealed) layers. For irradiation, laser sources operating at three wavelengths in band gap region of the studied materials were employed. The results show that lowest values of photorefraction accompanied with lowest changes of band gap values were exhibited by $Ge_{20}As_{20}Te_{60}$ thin films, which are therefore considered as the layers with highest photostability in relaxed state. The structure of the films is discussed based on Raman scattering spectroscopy data.

Amorphous chalcogenides based on S, Se and Te elements in combination with suitable element(s) from 14th or 15th group of the periodical system (typically Ge, As, etc.) are unique due to their photoinduced phenomena. Irradiation source of appropriate energy and intensity can change physico-chemical properties (refractive index, position of fundamental short-wavelength absorption edge, thickness, etc.) of amorphous chalcogenide thin films[1]. On the other hand, due to photoinduced changes of structure and properties, their potential applications in field of infrared optics, based on interesting nonlinear optical properties of amorphous chalcogenides have been limited[2].

On the basis of photoinduced phenomena knowledge in binary arsenic- and germanium-based amorphous chalcogenides[3–5], it would be supposed that in ternary Ge-As-Te(S, Se) materials, photodarkening (decrease of band gap energy) and photobleaching (increase of band gap energy), connected with positive or negative photorefraction (refractive index changes), could be compensated by an appropriate choice of composition. Nevertheless, the studies leading to optimization of intrinsic chemical composition of amorphous chalcogenides in order to prevent undesired photoinduced effects are rare[6–8], dealing with Ge-As-Se thin amorphous films. It is worthy to mention reported coexistence of fast photodarkening and slow photobleaching in thermally evaporated Ge-As-Se films[9,10] as well as transient absorption effects induced by nanosecond pulsed lasers[11].

Infrared transparency window of S- and Se-based amorphous chalcogenides is restricted by the long-wavelength (multiphonon) absorption edge at 11 and 15 μm, respectively[12]. However, for some applications, it is necessary to develop materials optically transparent beyond 16 μm. This requirement might be satisfied by use of amorphous tellurides, for example from binary Te-X (X = Cl, Br or I), Ge-Te, As-Te or ternary Ge-Ga-Te, Ge-Te-I, Ge-In-Te or Ge-As-Te systems[13,14]. Among mentioned systems, excellent optical transparency in the 3–20 μm spectral window as well as large refractive index values (>3.5 at 1.55 μm) were reported for Ge-As-Te glasses[14,15].

Based on interesting properties of bulk glasses and expectation of photostable thin films discovery, this work deals with amorphous thin films from Ge-As-Te system. In detail, the aim of this work is to find Ge-As-Te photostable thin films in as-deposited but preferably in relaxed (annealed) state. The term photostability can be defined as insensitivity of the material to light exposure in terms of constant values of refractive index and optical band gap.

Preparation of Ge-As-Te amorphous thin films using electron beam or flash evaporation was already reported[16,17]. In this work, we used pulsed laser deposition (PLD) for thin films growth. PLD technique seems to be promising for chalcogenide thin films fabrication due to its simplicity, easy control of the deposition process, possibility to fabricate multilayered structures and often stoichiometric material transfer from the target to the films[18,19].

Following our previous work in Ge-As-Se system[7,20], we studied photostability/photosensitivity and structure for six selected compositions from Ge-As-Te system employing three different laser sources having photon energy close to bandgap of the studied materials because amorphous chalcogenides are generally most sensitive for exposures with band gap light. Five compositions followed the trend of increasing mean coordination number (MCN) from 2.4 to 2.8; last composition ($Ge_{20}As_{20}Te_{60}$, MCN = 2.6) was chosen for a comparison with Ge-As-Se system studied recently.

Results

The thin films fabricated by PLD were amorphous and homogenous according XRD patterns (Fig. 1) and SEM (Fig. 2). The SEM and AFM found smooth surface of thin films, without cracks and corrugations (Fig. 2 and 3). We observed only rarely sub-micrometer sized droplets. Surface roughness (RMS) values of all thin films determined by AFM were found to be lower than ~1.7 nm (Table 1); no changes in surface roughness were indicated for annealed, irradiated and post-annealing irradiated layers.

The chemical composition of fabricated layers, as determined by SEM-EDS, is in good agreement with the composition of used bulk targets[15] (Table 1). The only exception is $Ge_{10}As_{60}Te_{30}$ composition, where the differences between thin film and bulk target composition are probably caused by non-homogeneity of the bulk material, which was partly crystalline. In spite of the fact that the bulk $Ge_{20}As_{20}Te_{60}$ target was completely crystalline (this composition is located outside the glass-forming region[21]), corresponding films were amorphous and their chemical composition agreed well with average composition of the used target.

Two series of $Ge_xAs_yTe_{100-x-y}$ thin films differing in thickness (~300 and ~1000 nm, Table 1) were fabricated in order to satisfy

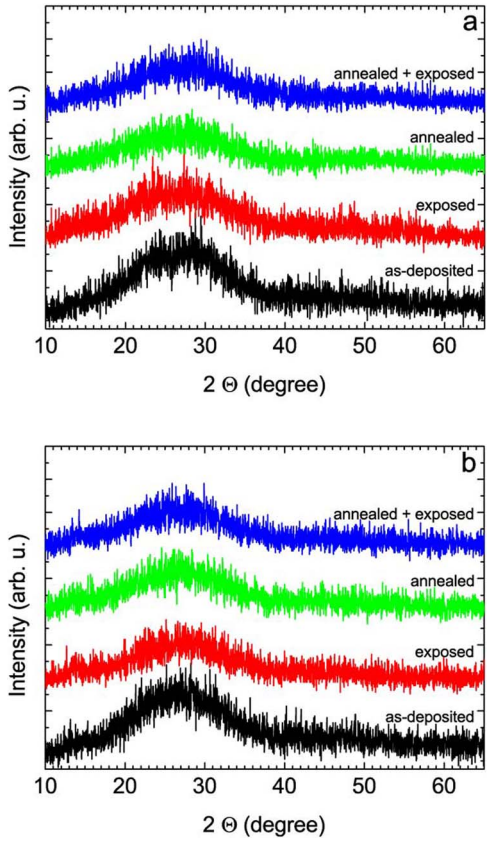

Figure 1 | XRD patterns of (a) $Ge_{10}As_{30}Te_{60}$ and (b) $Ge_{20}As_{20}Te_{60}$ thin films in different states of the samples (as-deposited, exposed at 1342 nm, annealed and post-annealing exposed at 1342 nm).

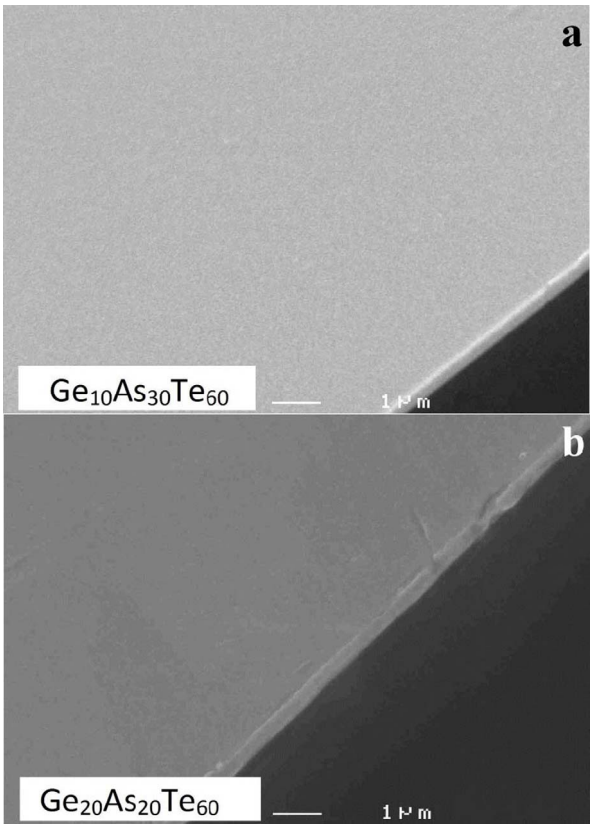

Figure 2 | SEM micrographs of (a) $Ge_{10}As_{30}Te_{60}$ and (b) $Ge_{20}As_{20}Te_{60}$ thin films.

criterion of penetration depth of the light sources used for the exposure experiments which must be equal or larger than the film thickness. The penetration depth for 1064 nm (1.17 eV) laser light was estimated to be 300–400 nm, laser beam of two other sources had penetration depth values larger than 2 μm. Because films with thickness around 300 nm were irradiated with 1064 nm (1.17 eV) and 1342 nm (0.92 eV) lasers and films with thickness around 1000 nm were exposed with 1342 nm (0.92 eV) and 1550 nm (0.80 eV) sources, above mentioned criterion was satisfied.

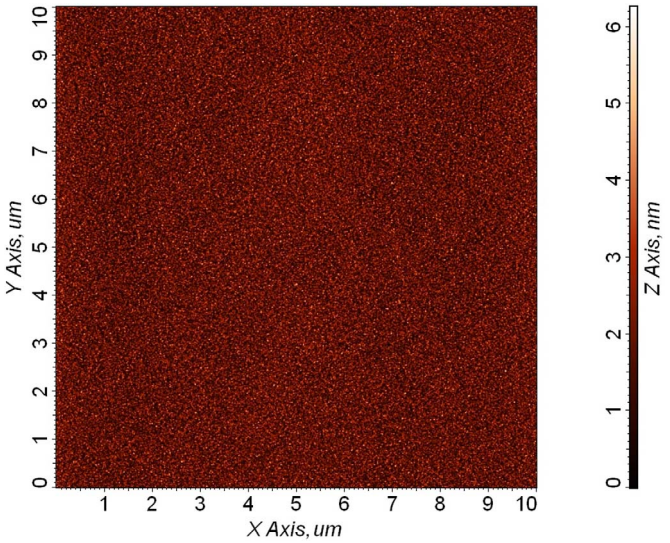

Figure 3 | AFM surface scan (10 μm × 10 μm, semicontact mode) of as-deposited $Ge_{10}As_{50}Te_{40}$ thin film.

Table 1 | Nominal and real chemical composition (from EDS, ± 0.5 at. %) of Ge-As-Te thin films. MCN and MCN* stand for the mean coordination numbers calculated from nominal composition and EDS results, respectively. Surface roughness RMS values were extracted from AFM data. Thicknesses of two series of fabricated thin films were determined by VASE data analysis (±2 nm)

Nominal composition	MCN	Ge (at. %)	As (at. %)	Te (at. %)	MCN*	Surface roughness (nm)	Thickness (nm)
$Ge_{10}As_{20}Te_{70}$	2.40	13.3	23.0	63.7	2.50	1.72 ± 0.15	280/1050
$Ge_{10}As_{30}Te_{60}$	2.50	11.6	30.1	58.2	2.53	1.06 ± 0.11	270/870
$Ge_{10}As_{40}Te_{50}$	2.60	12.2	38.6	49.2	2.63	1.05 ± 0.11	320/810
$Ge_{10}As_{50}Te_{40}$	2.70	10.3	50.9	38.8	2.72	0.89 ± 0.09	335/930
$Ge_{10}As_{60}Te_{30}$	2.80	14.1	46.0	39.9	2.74	1.08 ± 0.11	375/1000
$Ge_{20}As_{20}Te_{60}$	2.60	22.5	19.2	58.3	2.64	1.26 ± 0.12	330/1010

Transmission spectra of as-deposited Ge-As-Te thin films (Fig. 4, microscope glass substrates) show good quality of the layers with transmittance reaching 86% at interferences' maxima. Fig. 4 demonstrates also the position of short wavelength absorption edges of the layers in near infrared spectral region; specifically, the wavelengths where transmission is equal to 10% are located in 950–1000 nm range. For reader's convenience, Fig. 4 indicates also wavelengths of laser sources used for photosensitivity experiments.

The thicknesses, optical band gap and refractive indices of all thin films were determined by variable angle spectroscopic ellipsometry (VASE) data analysis. The applicability of Cody-Lorentz model for the VASE data analysis is confirmed by low values of mean square error (MSE) of the fitting procedure, typically MSE < 6.

Tables 2 and 3 show optical band gap values and refractive indices at 1540 nm for 300 nm PLD Ge-As-Te thin films in different states (as-deposited, exposed, annealed, post-annealing exposed). The data presented stand for irradiation with laser sources operating at 1064 nm (1.17 eV, super band gap light) and 1342 nm (0.92 eV, band gap light). For clarity, data obtained for 1000 nm films, which were exposed with laser sources operating at 1342 nm (band gap light) and 1550 nm (0.8 eV, sub band gap light), are not shown in Tables 2 and 3. Examples of refractive indices spectral dependences are illustrated in Figure 5.

The local structure of as-deposited, exposed, annealed and post-annealing exposed Ge-As-Te films was studied via analysis of Raman scattering spectroscopy data. The examples of thin films' Raman spectra of two selected compositions are given in Fig. 6. The Raman spectra are dominated by the most intensive band peaking at ~123 cm^{-1}, independent of the state of the sample. Other Raman bands' maxima are located at ~141, ~159, ~185–195 and ~220–230 cm^{-1}.

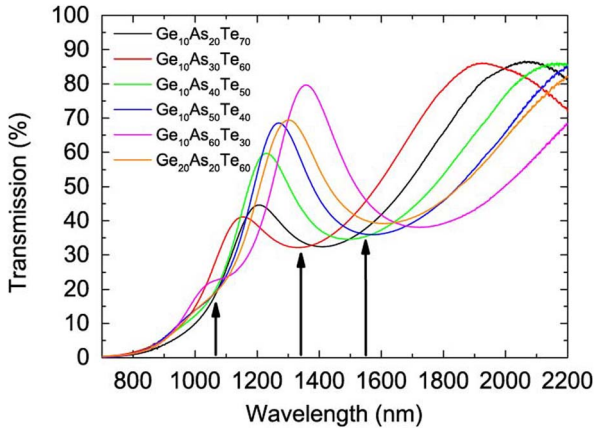

Figure 4 | Transmittance spectra of as-deposited Ge-As-Te thin films. Black arrows show wavelengths of laser sources used for photosensitivity experiments.

Discussion

From the obtained results, one can conclude that the irradiation of as-deposited Ge-As-Te layers leads to some photodarkening effect for ~300 nm thick films with nominal composition $Ge_{10}As_{20}Te_{70}$ (partly also $Ge_{10}As_{30}Te_{60}$); the photodarkening takes place for 0.92 eV irradiation (ΔE_g^{opt} up to ~0.11 eV). Under 1.17 eV exposure, films are photostable.

For ~1000 nm thick films, the impact of irradiation on as-deposited films has following trend. Under 0.92 eV irradiation, clear photobleaching was observed for most of the samples (ΔE_g^{opt} up to ~0.07 eV). On the other hand, under 0.8 eV irradiation, only weak photobleaching was detected for $Ge_{10}As_{40}Te_{50}$ and $Ge_{10}As_{50}Te_{40}$ layers (ΔE_g^{opt} up to ~0.04 eV), if any. Exposure of as-deposited Ge-As-Te films has generally only small effect on their refractive index values at 1540 nm, if any ($\Delta n \leq 0.02$).

The relaxation of as-deposited films via annealing in inert atmosphere generally results in their bleaching (ΔE_g^{opt} up to ~0.18 eV for $Ge_{10}As_{60}Te_{30}$), excluding 300 nm $Ge_{10}As_{20}Te_{70}$ layers which underwent darkening (ΔE_g^{opt} up to ~0.07 eV). The bleaching of as-deposited thin films due to annealing is connected with the decrease of refractive index (Δn up to ~0.16 in case of $Ge_{10}As_{60}Te_{30}$).

The behavior of relaxed (annealed) PLD Ge-As-Te amorphous thin films under exposure with different laser sources has not general trends (except the fact that no photobleaching was identified); that is why each composition will be commented separately. Two compositions ($Ge_{10}As_{50}Te_{40}$ and $Ge_{20}As_{20}Te_{60}$) exhibit almost completely photostable behavior of optical band gap in relaxed state. Relaxed $Ge_{10}As_{20}Te_{70}$ layers show photodarkening reaching ΔE_g^{opt} up to ~0.09 eV for 0.92 eV irradiation. Photodarkening was observed also for $Ge_{10}As_{30}Te_{60}$ relaxed films; ΔE_g^{opt} ~0.08 eV for 0.92 eV irradiation, magnitude of photodarkening is lower for two other irradiation sources. In case of $Ge_{10}As_{40}Te_{50}$ annealed films, photostability was found for 1.17 eV exposure; contrary, for 0.92 and 0.80 eV irradiation, weak photodarkening is reported. Finally, the photostability of $Ge_{10}As_{60}Te_{30}$ layers in relaxed state is rather good under 1.17 and 0.92 eV irradiation; however, under 0.80 eV exposure photodarkening with magnitude of ΔE_g^{opt} ~0.05 eV is seen. From the point of photorefraction, four studied compositions ($Ge_{10}As_{30}Te_{60}$, $Ge_{10}As_{40}Te_{50}$, $Ge_{10}As_{50}Te_{40}$ and $Ge_{20}As_{20}Te_{60}$) present almost zero photorefraction in relaxed state under all three irradiation sources.

Taking into account all the data, lowest values of photorefraction accompanied with lowest changes of band gap values were identified for $Ge_{20}As_{20}Te_{60}$ thin films, which are therefore considered as the layers with highest photostability among studied samples, especially in relaxed state. Zero photorefraction is of high importance for some applications of amorphous chalcogenides, such as for laser beam propagation in nonlinear regime[2]. That is why pulsed laser deposited $Ge_{20}As_{20}Te_{60}$ thin films are attractive and promising also due to their expected high (non)linear refractive index.

Discovery of thin films photostability in Ge-As-Te system, located at $Ge_{20}As_{20}Te_{60}$ composition (MCN = 2.6), is coherent with our earlier work dealing with Ge-As-Se amorphous layers, where the

Table 2 | Ge-As-Te thin films optical band gap values (in eV) at different stages of the experiments (as-deposited, exposed, annealed and post-annealing exposed). Band gap values were extracted from VASE data analysis (±0.01 eV). Note that data shown are for films with ~300 nm thickness. E_{irr} is the energy of laser light used for irradiation experiments

E_{irr}	1.17 eV				0.92 eV			
	as-deposited		annealed		as-deposited		annealed	
composition	non-irrad.	irradiated	non-irrad.	irradiated	non-irrad.	irradiated	non-irrad.	irradiated
$Ge_{10}As_{20}Te_{70}$	0.90	0.89	0.83	0.82	0.90	0.79	0.86	0.77
$Ge_{10}As_{30}Te_{60}$	0.90	0.91	0.94	0.89	0.89	0.84	0.96	0.88
$Ge_{10}As_{40}Te_{50}$	0.89	0.89	0.96	0.95	0.90	0.90	0.99	0.95
$Ge_{10}As_{50}Te_{40}$	0.89	0.92	1.00	1.00	0.90	0.90	1.00	1.01
$Ge_{10}As_{60}Te_{30}$	0.90	0.90	1.04	1.06	0.89	0.89	1.07	1.07
$Ge_{20}As_{20}Te_{60}$	0.89	0.88	1.02	1.01	0.90	0.89	1.01	1.00

photostable composition was found to be $Ge_{20}As_{20}Se_{60}$[7]. As pointed out by Calvez et al.[22], photostructural changes such as photodarkening decrease and tend to vanish in overcoordinated glasses, i.e. when MCN = 2.6 in Ge-As-Se system. In case of Ge-As-Te thin films studied here, some compositions have MCN higher than 2.6; however, they present some photoinduced phenomena. Moreover, $Ge_{10}As_{40}Te_{50}$ films having MCN = 2.6 are not completely photostable. Above mentioned facts lead to the conclusion that MCN does not seem to be the main decisive parameter influencing photostability of amorphous chalcogenides. Our conclusion is supported by the work of Khan et al., who studied light induced response of thermally evaporated Ge-As-Se thin films concluding that coexisting photodarkening and photobleaching do not show a regular trend with respect to MCN; instead evidence that Ge: As ratio plays important role, rather than rigidity of the amorphous network, is provided[10].

In an earlier work, Tanaka[23] claimed that the band gap (and super band gap) irradiation affects with higher efficiency lone pair electrons of chalcogen atoms (which are supposed to be responsible for photoinduced phenomena) than the sub band gap light. Our results do not correlate completely with this statement.

Usually, changes of optical parameters are accompanied by structural changes. Generally, it is known that telluride films are easy to crystallize (which can also lead to changes in optical properties) in comparison with selenide/sulfide layers[24]. XRD patterns (Fig. 1) show that studied Ge-As-Te films are amorphous in different states of the samples (as-deposited, exposed, annealed and post-annealing exposed). Thus, no phase change of studied telluride thin films is observed under exposure/annealing.

To have deeper insight into the structure of the Ge-As-Te films, Raman scattering spectra for all states of the layers were measured as illustrated in Fig. 6. We discuss first the Raman spectra of as-deposited films. Raman band peaking at ~123 cm^{-1} can be assigned to vibrations of $GeTe_4$ tetrahedra (A_1 symmetric stretching mode), $GeTe_{4-n}Ge_n$ (n = 1, 2) corner-sharing tetrahedra (A_1 mode)[25] and symmetric bending vibrations of $AsTe_3$ pyramids (A_1 mode)[26]. The Raman band with maximum at ~141 cm^{-1} could be attributed to vibrations of short Te disordered chains as in amorphous tellurium (experimentally observed at ~157 cm^{-1}), where the vibration frequency is shifted due to long range interaction between the chains[27]. The 141 cm^{-1} peak can be also connected with the E mode (anti-symmetric stretching) in crystalline Te[26,28]. It should be mentioned that the α-GeTe shows Γ_1 phonon mode at 140 cm^{-1} [29]. As the trigonal Te has the main Raman active A_1 symmetric stretching mode at 120 cm^{-1}, the Raman band at 123 cm^{-1} observed in Ge-As-Te films may have a mixed character with some contribution from Te–Te vibrations as well[26,28]. The Raman band with maximum at ~159 cm^{-1} has been attributed to the anti-symmetric bending vibrations of $AsTe_3$ pyramids (E mode)[26], A_1 mode of $GeTe_4$ edge-sharing tetrahedra[25] and/or Te-Te vibrations as in amorphous tellurium (disordered chains)[27]. Further, we connect the Raman band peaking at ~185–195 cm^{-1} to A_1 mode of $GeTe_{4-n}Ge_n$ (n = 1, 2) edge-sharing tetrahedra vibrations[25]. We cannot exclude a contribution (to the band peaking at ~185–195 cm^{-1}) coming from vibrations of distorted octahedral $GeTe_3$ units in analogy with work of Voleská et al.[30] Finally, very weak Raman band (shoulder) with maxima located at ~220–230 cm^{-1} can be associated with F_2 mode of $GeTe_{4-n}Ge_n$ tetrahedra anti-symmetric stretching vibrations[25]. In case of thin films with high arsenic content, it is necessary to take into account the presence of structural motifs rich in arsenic. Therefore we partly attribute the Raman bands peaking at 185–195 and ~220–230 cm^{-1} to symmetric (A_1 mode) and anti-symmetric (E mode) stretching vibrations of arsenic pyramids, respectively, in analogy with Ref[26].

The irradiation of as-deposited Ge-As-Te films has almost no effect on Raman spectra (Fig. 6). The annealing of as-deposited layers leads to small decrease of amplitudes of Raman bands peaking at

Table 3 | Refractive indices (at 1540 nm) of Ge-As-Te thin films at different stages of the experiments (as-deposited, exposed, annealed and post-annealing exposed). Refractive indices were extracted from VASE data analysis (±0.01). Note that data shown are for films with ~300 nm thickness. E_{irr} is the energy of laser light used for irradiation experiments

E_{irr}	1.17 eV				0.92 eV			
	as-deposited		annealed		as-deposited		annealed	
composition	non-irrad.	irradiated	non-irrad.	irradiated	non-irrad.	irradiated	non-irrad.	irradiated
$Ge_{10}As_{20}Te_{70}$	3.77	3.77	3.75	3.74	3.76	3.76	3.75	3.74
$Ge_{10}As_{30}Te_{60}$	3.72	3.73	3.68	3.66	3.69	3.68	3.67	3.66
$Ge_{10}As_{40}Te_{50}$	3.70	3.69	3.61	3.62	3.71	3.70	3.61	3.62
$Ge_{10}As_{50}Te_{40}$	3.69	3.70	3.60	3.58	3.70	3.69	3.59	3.57
$Ge_{10}As_{60}Te_{30}$	3.66	3.65	3.53	3.50	3.68	3.66	3.52	3.52
$Ge_{20}As_{20}Te_{60}$	3.62	3.62	3.52	3.51	3.63	3.63	3.53	3.52

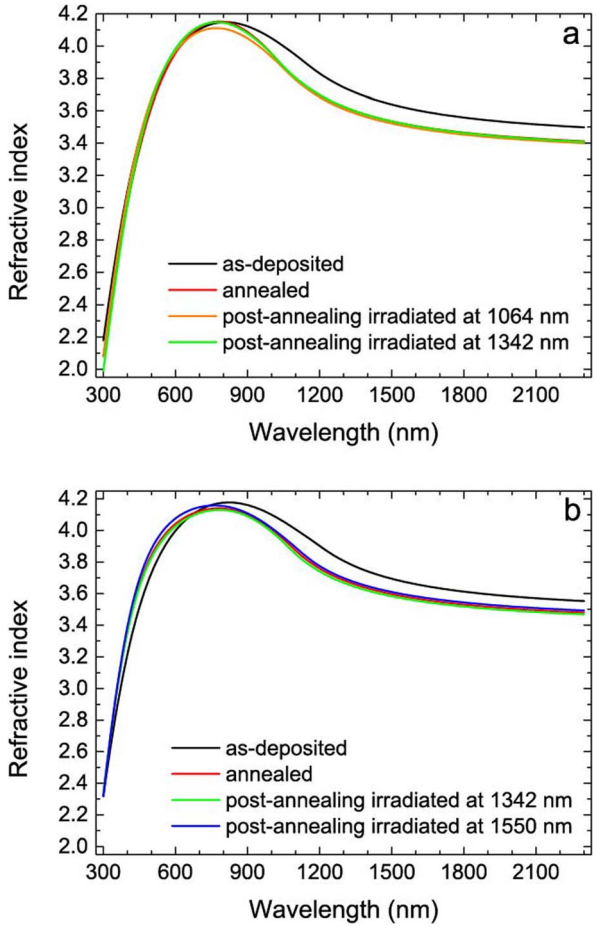

Figure 5 | Refractive indices spectral dependences (calculated from VASE data analysis, error in determination ± 0.01) for 300 nm $Ge_{20}As_{20}Te_{60}$ (a) and 1000 nm $Ge_{10}As_{50}Te_{40}$ (b) thin films.

~123 and 141 cm^{-1}. At the same time, amplitudes of Raman bands with maxima at ~159 and 185–195 cm^{-1} slightly increase. Depicted changes may be mainly connected with the slight increase of content of edge-sharing $GeTe_{4-n}Ge_n$ ($n = 0, 1, 2$) tetrahedra at the expense of corner-sharing ones. We cannot exclude that also some changes in ordering of short Te chains proceed on annealing. Post-annealing exposure leads to different effects. In case of films considered as photostable (especially $Ge_{20}As_{20}Te_{60}$), no changes of Raman spectra were identified between annealed and post-annealing exposed states (Fig. 6). On the other hand, films which are photosensitive present some changes in Raman spectra, qualitatively similar to changes on annealing (small amplitudes' decrease of bands peaking at ~123 and 141 cm^{-1}, slight increase of bands peaking at ~159 and 185–195 cm^{-1}). This observation leads to the conclusion that irradiation of relaxed, but photosensitive Ge-As-Te films reflects in structural changes regarding slight increase of content of edge-sharing $GeTe_{4-n}Ge_n$ ($n = 0, 1, 2$) tetrahedra at the expense of corner-sharing ones.

It should be mentioned that a phenomenological description of the photoinduced effects in amorphous chalcogens and chalcogenides is often given by configuration-coordinate models[1,23,31], which propose the ground state of the system formed by a double-well potential with an energy barrier separating the ground and metastable states. After the photoexcitation, the system is transferred to the metastable state, where (after electronic relaxation), the electron and hole are trapped in the conduction-band tail state and in the valence-band edge state, respectively. In case that the distance between the electron and the hole is too long for immediate recombination, a polaron like structural change takes place. After the structural change, the carriers recombine and the structure is frozen, being more disordered. More disordered amorphous structure is connected with more random interlayer distances (van der Waals forces) leading to an increase of valence band broadening followed by the photodarkening and the refractive index rise.

Unfortunately, above mentioned configurational models cannot explain microscopic origin of the photoinduced effects resulting in volume changes. It is worthy to remind models of photoinduced volume changes proposed by Shimakawa[32], Tanaka[33] and Yang[34]. Shimakawa assumes macroscopic carrier diffusion and Coulomb repulsion among the layer fragments. Tanaka proposes the chalcogen atom bonds twisting with interlayer relaxation enhancing fluidity. Yang's model is based on bond angle increase and wrong bond creation. A model explaining both photoinduced expansion and contraction in both glassy and partly crystallized chalcogenides

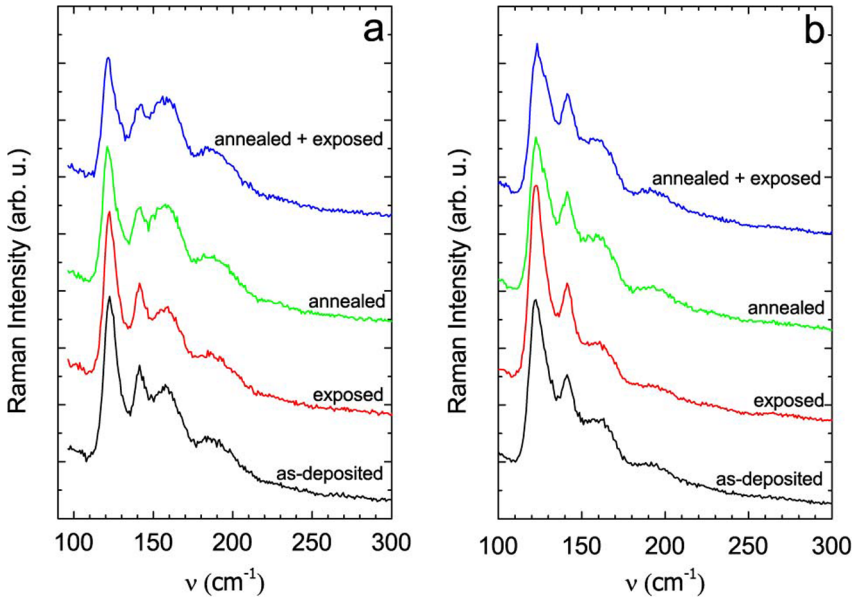

Figure 6 | Raman scattering spectra of (a) $Ge_{10}As_{30}Te_{60}$ and (b) $Ge_{20}As_{20}Te_{60}$ thin films in different states of the samples (as-deposited, exposed at 1342 nm, annealed and post-annealing exposed at 1342 nm).

which involves Coulombic repulsive interaction (causing volume expansion) as well as cross-linking of molecular units through bond-switching (leading to volume contraction) was introduced by Chen[35]. It should be noted that no general, quantitative model is available at present time.

Nevertheless, as no clear trends in thicknesses changes of the Ge-As-Te films under irradiation were observed, we believe that the configuration-coordinate model is applicable in studied films. In order to better understand the phenomena observed in studied Ge-As-Te thin films, we envisage the measurements of transient photo-induced effects in near future.

In summary, pulsed laser deposition was exploited for the fabrication of Ge-As-Te amorphous thin films. Morphology of prepared films is of good quality and their surface roughness is low. Photostability of the layers was studied in as-deposited as well as annealed state of the samples under irradiation with lasers operating at 1064, 1342 and 1550 nm. In studied Ge-As-Te thin films, no phase change occur upon annealing/exposure as proved by XRD patterns. As observed by Raman scattering spectroscopy, the annealing/post-annealing exposure leads only to marginal structural effects, resulting in slight increase of edge-sharing $GeTe_{4-n}Ge_n$ ($n = 0, 1, 2$) tetrahedra content at the expense of corner-sharing ones. Highest photostability connected with structural stability was found for $Ge_{20}As_{20}Te_{60}$ thin films, which are therefore promising for nonlinear applications.

Methods

Samples preparation. The targets used for PLD were bulk $Ge_xAs_yTe_{100-x-y}$ chalcogenide materials with nominal composition $Ge_{10}As_{20}Te_{70}$, $Ge_{10}As_{30}Te_{60}$, $Ge_{10}As_{40}Te_{50}$, $Ge_{10}As_{50}Te_{40}$, $Ge_{10}As_{60}Te_{30}$ (i.e. x = 10, y = 20, 30, 40, 50, 60) and $Ge_{20}As_{20}Te_{60}$ (i.e. x = 20, y = 20). Bulk samples were prepared by weighting high purity elements (5–6 N) in fused silica ampoules which were evacuated for a few hours and sealed subsequently. The sealed ampoules were heated in a rocking furnace at 1050°C for 12 hours and then quenched in water. Finally, glass rods were cut and polished for targets useful for PLD.

Thin films fabrication. For fabrication of thin films, a KrF excimer laser operating in UV (248 nm) was used. The laser pulses had constant output energy of 300 ± 3 mJ per pulse, 30 ns pulse duration and 20 Hz repetition rate. The energy fluency was set at ~2.6 J.cm^{-2}. Vacuum chamber (residual pressure $< 3 \times 10^{-4}$ Pa) was used for the fabrication of thin films; substrates were chemically cleaned microscope glass slides and Si wafers. The substrates were positioned parallel to the target at target-to-substrate distance of 5 cm. Off-axis PLD technique with rotating target and substrates was used to avoid deep damage of the target and to improve the thickness homogeneity of deposited thin films.

Photostability experiments. Photostability was studied with as-deposited and annealed thin films. The annealing was realized in inert atmosphere of pure argon; annealing temperature was 20°C below the respective glass transition temperature of the corresponding target glass[15]. The duration of annealing was 120 min; the samples were consequently slowly cooled down to room temperature at 1°C.min^{-1}. The photostability experiments were performed via exposure of thin films by laser sources operating at 1064 nm (1.17 eV), 1342 nm (0.92 eV) and 1550 nm (0.80 eV) with intensity of ~160 mW.cm^{-2} for exposure time long enough (120 min) for the saturation of the photoinduced phenomena, if any. Laser exposures were realized in inert nitrogen atmosphere to avoid the oxidation of the films during the experiments.

Morphological, compositional and structural characterization. A scanning electron microscope with energy-dispersive X-ray analyzer (SEM-EDS, JSM 6400-OXFORD Link INCA) was used for chemical composition determination of prepared Ge-As-Te films. SEM technique was also applied to observe the morphology of thin films using a field-emission gun SEM (JMS 6301F). X-ray diffraction (XRD) technique (D8-Advance diffractometer, Bruker AXS) was exploited to prove amorphous state of thin layers using Bragg–Brentano θ–θ geometry with CuKα radiation and secondary graphite monochromator. The diffraction angles were measured at room temperature from 5 to 65° (2θ) in 0.02° steps with a counting time of 5 s per step. The Raman scattering spectra of studied films were measured at room temperature by LabRAM HR spectrometer (Horiba Jobin-Yvon) with 785 nm laser as excitation source. The intensity of laser beam was kept at low level to avoid thermally induced structural transformations resulting from absorption of high laser power densities. The frequency resolution of used configuration was ~0.7 cm^{-1} per pixel. Atomic force microscopy (AFM, Solver NEXT, NT-MDT) was used to study topography of Ge-As-Te thin films within typical scanned area 10 μm × 10 μm in semicontact mode.

Optical characterization. Transmittance spectra of as-deposited thin films were measured using Shimadzu UV-3600 spectrophotometer in 700–2200 nm spectral range. Optical functions (refractive indices and extinction coefficient spectral dependences) and thicknesses of $Ge_xAs_yTe_{100-x-y}$ thin films were obtained from the analysis of spectroscopic ellipsometry data measured using an ellipsometer with automatic rotating analyzer (VASE, J.A. Woollam Co., Inc.). The measurement parameters are as follows: spectral region 300–2300 nm with 10 or 20 nm steps (depending on thickness of the films), angles of incidence 50°, 60° and 70°. For the analysis of VASE data we used Cody-Lorentz model[36], which includes the correct band edge function, weak Urbach absorption tail description as well as Lorentz oscillator function; this model is appropriate for the description of amorphous chalcogenides optical functions and their photo-induced changes[7]. VASE data were fitted by a set of three parameters describing the Lorentz oscillator (A – Lorentz oscillator amplitude (oscillator strength), E_0 – resonance (peak transition) energy, Γ – oscillator width (broadening)) and four parameters describing band edge function (E_t – demarcation energy between the Urbach tail transition and the band-to-band transition, E_u – Urbach energy, E_g^{opt} – optical band gap energy, E_p – transition energy separating the absorption onset from Lorentz oscillator behavior). Finally, thicknesses of the thin films, thicknesses uniformity and thicknesses of surface roughness layer (modeled by effective medium approximation) were fitting parameters as well.

1. Shimakawa, K., Kolobov, A. & Elliott, S. R. Photoinduced effects and metastability in amorphous semiconductors and insulators. *Adv. Phys.* **44**, 475–588 (1995).
2. Chauvet, M. *et al.* Kerr spatial solitons in chalcogenide waveguides. *Opt. Lett.* **34**, 1804–1806 (2009).
3. Nemec, P., Nazabal, V. & Frumar, M. Photoinduced phenomena in amorphous As_4Se_3 pulsed laser deposited thin films studied by spectroscopic ellipsometry. *J. Appl. Phys.* **106**, 023509 (2009).
4. Sleeckx, E., Tichy, L., Nagels, P. & Callaerts, R. Thermally and photo-induced irreversible changes in the optical properties of amorphous Ge_xSe_{100-x} films. *J. Non-Cryst. Solids* **200**, 723–727 (1996).
5. Vateva, E. Giant photo- and thermo-induced effects in chalcogenides. *J. Optoelectron. Adv. Mater.* **9**, 3108–3114 (2007).
6. Yang, G. *et al.* A photo-stable chalcogenide glass. *Opt. Express* **16**, 10565–10571 (2008).
7. Nemec, P. *et al.* Photo-stability of pulsed laser deposited $Ge_xAs_ySe_{100-x-y}$ amorphous thin films. *Opt. Express* **18**, 22944–22957 (2010).
8. Su, X., Wang, R., Luther-Davies, B. & Wang, L. The dependence of photosensitivity on composition for thin films of $Ge_xAs_ySe_{1-x-y}$ chalcogenide glasses. *Appl. Phys. A-Mater. Sci. Process.* **113**, 575–581 (2013).
9. Khan, P. *et al.* Coexistence of fast photodarkening and slow photobleaching in $Ge_{19}As_{21}Se_{60}$ thin films. *Opt. Express* **20**, 12416–12421 (2012).
10. Khan, P., Jain, H. & Adarsh, K. V. Role of Ge: As ratio in controlling the light-induced response of a-$Ge_xAs_{35-x}Se_{65}$ thin films. *Sci. Rep.* **4**, 4029 (2014).
11. Khan, P., Saxena, T., Jain, H. & Adarsh, K. V. Nanosecond light induced, thermally tunable transient dual absorption bands in a-$Ge_5As_{30}Se_{65}$ thin film. *Sci. Rep.* **4**, 6573 (2014).
12. Eggleton, B. J., Luther-Davies, B. & Richardson, K. Chalcogenide photonics. *Nature Photonics* **5**, 141–148 (2011).
13. Bureau, B. *et al.* Tellurium based glasses: A ruthless glass to crystal competition. *Solid State Sci.* **10**, 427–433 (2008).
14. Yang, Z. Y. & Lucas, P. Tellurium-based far-infrared transmitting glasses. *J. Am. Ceram. Soc.* **92**, 2920–2923 (2009).
15. Hawlová, P., Verger, F., Nazabal, V., Boidin, R. & Němec, P. Accurate determination of optical functions of Ge–As–Te glasses via spectroscopic ellipsometry. *J. Am. Ceram. Soc.* **97**, 3044–3047 (2014).
16. Mohamed, S. H., Wakkad, M. M., Ahmed & Diab, A. M. Structural and optical properties of Ge-As-Te thin films. *The European Physical Journal Applied Physics* **34**, 165–171 (2006).
17. Pinto, R. Threshold and memory switching in thin films of the chalcogenide systems Ge-As-Te and Ge-As-Se. *Thin Solid Films* **7**, 391–404 (1971).
18. Nemec, P., Takats, V., Csik, A. & Kokenyesi, S. GeSe/GeS nanomultilayers prepared by pulsed laser deposition. *J. Non-Cryst. Solids* **354**, 5421–5424 (2008).
19. Nemec, P. *et al.* Pulsed laser deposited amorphous chalcogenide and alumino-silicate thin films and their multilayered structures for photonic applications. *Thin Solid Films* **539**, 226–232 (2013).
20. Hawlova, P., Olivier, M., Verger, F., Nazabal, V. & Nemec, P. Photosensitivity of pulsed laser deposited $Ge_{20}As_{20}Se_{60}$ and $Ge_{10}As_{30}Se_{60}$ amorphous thin films. *Mater. Res. Bull.* **48**, 3860–3864 (2013).
21. Krebs, H. & Fischer, P. Electrical conductivity of melts and their ability to form glasses in the system Ge + As + Te. *Discussions of the Faraday Society* **50**, 35–44 (1970).
22. Calvez, L., Yang, Z. Y. & Lucas, P. Light-induced matrix softening of Ge-As-Se network glasses. *Phys. Rev. Lett.* **101**, 177402 (2008).
23. Tanaka, K. *Photo-Induced Metastability in Amorphous Semiconductors* [Kolobov, A. V. (ed.)] [69–90] (Wiley-WCH, Weinheim, 2003).
24. Wuttig, M. & Raoux, S. The science and technology of phase change materials. *Z. Anorg. Allg. Chem.* **638**, 2455–2465 (2012).
25. Andrikopoulos, K. S. *et al.* Raman scattering study of the a-GeTe structure and possible mechanism for the amorphous to crystal transition. *J. Phys.: Condens. Matter* **18**, 965–979 (2006).

26. Sen, S., Gjersing, E. L. & Aitken, B. G. Physical properties of $Ge_xAs_{2x}Te_{100-3x}$ glasses and Raman spectroscopic analysis of their short-range structure. *J. Non-Cryst. Solids* **356**, 2083–2088 (2010).
27. Brodsky, M. H., Smith, J. E., Yacoby, Y. & Gambino, R. J. Raman spectrum of amorphous tellurium. *Phys. Status Solidi B-Basic Res.* **52**, 609–614 (1972).
28. Pine, A. S. & Dresselhaus, G. Raman spectra and lattice dynamics of tellurium. *Phys. Rev. B* **4**, 356–371 (1971).
29. Steigmeier, E. F. & Harbeke, G. Soft phonon mode and ferroelectricity in GeTe. *Solid State Commun.* **8**, 1275–1279 (1970).
30. Voleska, I. *et al.* Structure, electronic, and vibrational properties of glassy $Ga_{11}Ge_{11}Te_{78}$: Experimentally constrained density functional study. *Phys. Rev. B* **86**, 094108 (2012).
31. Kolobov, A. V. & Tanaka, K. *Handbook of Advanced Electronic and Photonic Materials and Devices* Vol. 5 [Nalwa, H. S. (ed.)] [47–85] (Academic Press, London, 2001).
32. Shimakawa, K., Yoshida, N., Ganjoo, A., Kuzukawa, Y. & Singh, J. A Model for the Photostructural Changes in Amorphous Chalcogenides. *Philos. Mag. Lett.* **77**, 153–158 (1998).
33. Tanaka, K. Sub-gap excitation effects in As_2S_3 glass. *J. Non-Cryst. Solids* **266**, 889–893 (2000).
34. Yang, C. Y., Paesler, M. A. & Sayers, D. E. Measurement of local structural configurations associated with reversible photostructural changes in arsenic trisulfide films. *Phys. Rev. B* **36**, 9160–9167 (1987).
35. Chen, G., Jain, H., Vlcek, M. & Ganjoo, A. Photoinduced volume change in arsenic chalcogenides by band-gap light. *Phys. Rev. B* **74**, 174203 (2006).
36. Cody, G. D. *Semiconductors and Semimetals* Vol. 21, Part B [Pankove, J. I. (ed.)] [11–82] (Academic Press, London, 1984).

Acknowledgments

The Czech Science Foundation (Project No. 13-05082S), Ministry of Education, Youth and Sports of the Czech Republic (Project CZ.1.07/2.3.00/30.0058) and the CNRS PICS (Projet International de Cooperation Scientifique) program financially supported this work. Authors are grateful to Dr. L. Beneš and Prof. Z. Černošek for XRD and Raman scattering spectroscopy measurements, respectively.

Author contributions

P.N. conceived the idea. P.H. made the samples. P.H., F.V., V.N. and R.B. did the experiments. P.H., R.B. and P.N. analyzed the data. All authors wrote and reviewed the manuscript.

Additional information

Competing financial interests: The authors declare no competing financial interests.

How to cite this article: Hawlová, P., Verger, F., Nazabal, V., Boidin, R. & Němec, P. Photostability of pulsed laser deposited amorphous thin films from Ge-As-Te system. *Sci. Rep.* **5**, 9310; DOI:10.1038/srep09310 (2015).